Korean J. Chem. Eng., 32(9), 1910-1917 (2015)
DOI: 10.1007/s11814-014-0384-9

pISSN: 0256-1115
eISSN: 1975-7220

Controlling the polymorphism of carbamazepine-saccharin cocrystals formed during antisolvent cocrystallization using kinetic parameters

Min-Jeong Lee*,‡, In-Chun Wang*,‡,‡, Min-Ju Kim*, Paul Kim*, Keon-Hyoung Song*, Nan-Hee Chun, Hwa-Gyoo Park***, and Guang Jin Choi*,**,†**

*Department of Pharmaceutical Engineering, Soonchunhyang University, Asan, Chungnam, Korea
**Department of Biomedical Science, Soonchunhyang University, Asan, Chungnam, Korea
***Department of Health Administration & Management, Soonchunhyang University, Asan, Chungnam, Korea
(*Received 19 November 2014 • accepted 20 December 2014*)

Abstract−The cocrystal approach has been extensively investigated over the last decade as one of the most promising methods toward modifying the dissolution behavior of insoluble drug substances. This study demonstrates that the polymorphism of pharmaceutical cocrystalline powders prepared via antisolvent methods can be controlled using kinetic parameters. A carbamazepine-saccharin (CBZ-SAC) cocrystal was selected as a model drug in this study. This crystal was manufactured through a scaled-up antisolvent process with a total solution volume of 4.5 L. CBZ-SAC cocrystal crystalline powders were synthesized by adding 3 L of water as the antisolvent into 1.5 L of CBZ and SAC in methanol, whereby the antisolvent addition rate and the agitation speed were varied as the principal kinetic parameters. To investigate how cocrystallization proceeds under each condition, periodical sampling was combined with off-line characterization and in-line near-infrared (NIR) measurements to monitor the progress of reaction over the 120-minute process. We found that the creation of form-I was preferred when the addition speed or agitation speed was increased, but a highly pure form-II resulted if kinetic conditions were reversed. These differences in polymorphism can be explained by changes in kinetic characteristics when the process is monitored by NIR. This study is directly applicable to the industrial synthesis of these types of materials, precisely when specific CBZ-SAC cocrystalline polymorphs must be manufactured on a large scale.

Keywords: Co-crystal, Carbamazepine, Anti-solvent, Scale-up, Near-infrared, In-line Monitoring, Kinetic Parameter

INTRODUCTION

The potential for using a cocrystal approach toward improving key pharmaceutical attributes such as dissolution and the stability of crystalline compounds such as BCS Class-II drug substances has prompted a great deal of research into these methods. Recently, the US Food and Drug Administration (FDA) finalized guidelines for industry on pharmaceutical cocrystal methods [1]; additionally, the US FDA ruled that new cocrystal entities could be protected as intellectual property, based on their novelty and utility. These developments have spurred numerous overviews and reviews on the subject [2-6].

Traditionally, pharmaceutical cocrystals are prepared either by solid-state grinding (neat and wet) or solution (evaporation and cooling) methods [3,6]. The former approach has been recognized for its cocrystal screening capability and environmental benefits. Several cocrystallization methods are currently utilized, including the supercritical fluid method [7], solvent-mediated phase transformation (SMPT) [8], and ultrasound-assisted processing [9]. Previous studies comparing different methods found that spray-drying approaches produce pure cocrystal powders, even under incongruent saturating conditions, whereas solvent evaporation produces a mixture of cocrystal and individual components [10]. In this study, the formation of cocrystals was suggested to be kinetically controlled and mediated by the glassy state of materials during spray drying.

Previously, a novel thermodynamic-based screening method for carbamazepine (CBZ)-containing cocrystals was reported [11]. The ability to screen cocrystals promoted new methods of synthesizing novel cocrystals of CBZ. Additionally, a cocktail grinding method was explored as a potential screening tool for pharmaceutical cocrystals [12], allowing for the production of novel CBZ cocrystals more efficiently than a conventional one-at-a-time approach. Additional studies also showed that unusual cocrystals or cocrystal polymorphs could be produced by fast evaporation [13], whereby crystallization kinetics can be controlled by rapid solvent evaporation, increasing the chances of creating additional metastable crystalline forms. For example, the form-II polymorph of a CBZ-saccharin (SAC) cocrystal had not been synthesized before this study, except via a polymer-assisted heteronucleation approach [14].

Additional studies combined differential scanning calorimetry (DSC) and Fourier transform infrared (FTIR) spectroscopy into one step to screen cocrystal formation, including CBZ, in KBr pellets [15]. The true solubility of cocrystals is difficult to measure,

†To whom correspondence should be addressed.
E-mail: guangchoi@sch.ac.kr
‡These two authors equally made significant contribution to this study.
‡Current address: Unimed Pharm Inc., Asan, Chungnam, Korea

especially for highly soluble species, primarily due to transformation in solution. Noting this difficulty, a method to estimate the solubility of cocrystals, including CBZ, has been proposed based on equations predicting solubility [16]. Many analytical tools have been used to measure the characteristics of CBZ-containing cocrystals, including rapid-heating DSC to isolate and characterize the metastable CBZ-NCT form-II by fast heating of a CBZ-NCT glass at 400-500 °C/min [17] Different polymorphs of CBZ-containing cocrystals were produced through this method, depending on the type of milling employed [18]. This cocrystallization method has improved the dissolution profile and suspension stability when compared to commercially available immediate-release products.

Solvent mixtures were previously reported to drive CBZ-containing cocrystallization selectively by suppressing solvation formation in ultrasound-assisted solution reactions [19]; the success of this process increases with the number of solvents included in the mixture. A membrane-based crystallization technology was proposed to produce CBZ-SAC cocrystals directly from a water/ethanol solvent mixture [20,21]. In this process, ethanol is evaporated through 0.2-m filter pores to create a supersaturated state for the component solution. Once the optimal composition was attained, the selective production of CBZ and SAC crystals, as well as CBZ-SAC cocrystals, was achieved. Additionally, a scalable solution-cooling route using CBZ and nicotinamide has been reported [22]. This overall methodology consists of three key elements: solvent selection, selecting thermodynamic stability domains in a solid-liquid phase equilibrium diagram, and clarifying the kinetic processes for controlled desaturation.

Recently, we demonstrated the feasibility of using an antisolvent approach to prepare highly pure CBZ-SAC cocrystals [23], as well as indomethacin-saccharin cocrystal powders [24,25]. In a subsequent scale-up study, we found that the two known polymorphs (form-I and -II) of the CBZ-SAC cocrystal can be selected by controlling the experimental kinetic parameters. Very recently, comparative research concerning the spherical cocrystallization of CBZ and SAC was reported [26]. The primary aims of this study were to perform a 30-fold scale-up experiment of CBZ-SAC antisolvent cocrystallization and to propose a reasonable mechanism of cocrystal formation. In-line and off-line characterization (including IR spectroscopy) was used to monitor the progress of the reaction.

EXPERIMENTAL

1. Materials

Carbamazepine (CBZ; 5H-dibenzo[b,f]azepine-5-carboxamide) and saccharin (SAC; 2-benzothiazol-1,1,3-trione) powders were purchased from Sigma-Aldrich (St. Louis, MO, USA). Methanol, the solvent for both components was supplied as "reagent grade" by Merck Millipore (EMSURE®, Darmstadt, Germany) and used without further purification. Deionized water was used as the antisolvent and deionized as per purified water requirements set out by the US Pharmacopoeia (Human Corp., Seoul, Korea).

2. Antisolvent Cocrystallization

This experiment was based on previous research [23], with the work presented here scaling up this preceding research ~30 times. To keep the solvent:antisolvent volume ratio constant, 3 L of water was added to 1.5 L of CBZ and SAC in methanol at 25 °C using a peristaltic pump. Fig. 1 illustrates the experimental setup used in this study; the detailed procedure and instrumental information was previously reported [23]. The molar ratio of SAC to CBZ was fixed at 1.6 by holding the CBZ concentration at 0.075 M and the SAC concentration at 0.12 M. Among the various process parameters, the antisolvent addition rate and the agitation speed were examined as two critical kinetic parameters. Three levels were selected for each parameter: 100, 300, and 900 mL/min for the water addition rate, and 150, 300, and 600 rpm for the impeller agitation speed. Each reaction was left for 2 hours for each parameter, and the final solution was filtered via aspiration (using 2.5-mm-grade filter papers; Whatman, Maidstone, Kent, UK). Collected solids were dried in a vacuum oven at 25 °C overnight prior to subsequent characterization.

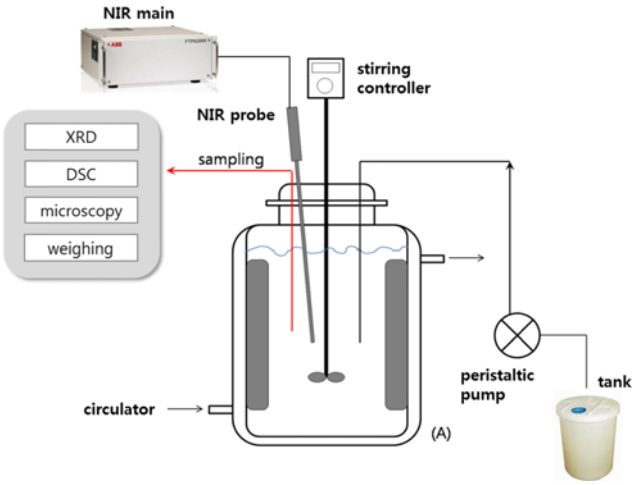

Fig. 1. Experimental setup for the antisolvent cocrystallization process (4.5-L scale).

3. Powder Characterization

The crystalline structures of synthesized powders were determined using a powder X-ray diffractometer (PXRD; DMAX-2200, Rigaku, Tokyo, Japan) with a Cu Kα radiation source (λ=1.54 A at 40 kV/40 mA). The PXRD pattern for each powder sample was acquired at a Bragg angle (2θ) of 5.30°, with a step size of 0.05° and a count time of 3 seconds per step. Thermal analyses were performed using DSC (DSC-60, Shimadzu, Otsu, Japan). Each specimen (5 mg) was loaded in an aluminum pan along with a empty pan as a reference, and DSC measurements were performed at 30-250 °C with a 10 °C/min heating rate under a nitrogen atmosphere. Solid powder morphology was observed under an optical microscope (CKX 41, Olympus, Tokyo, Japan).

To compare the thermal stability of cocrystal materials in the two-polymorph forms (form-I and form-II), crystal structures were examined at 70 °C. Fully dried cocrystal materials were stored in a drying oven at 70 °C for 4 weeks, and the stability of these heat-treated crystals was then measured using XRD and DSC.

4. Monitoring the Cocrystallization Process Using NIR Spectroscopy

The antisolvent cocrystallization reaction was performed under each kinetic condition for 2 hours. In-line NIR-based monitoring was conducted throughout the crystallization process, in addition

to intermittent sampling throughout crystallization to monitor the process via optical microscopy, XRD, and DSC. The first sample was taken when nucleation was observed, which occurred when the solution became turbid (as observed by the naked eye; 3-8 minutes). During each sampling period, 10 mL of solution was rapidly filtered using a vacuum filtering system prior to oven-drying. Each experimental condition was duplicated to evaluate reproducibility.

The NIR spectrometer (FTPA 2000-260; ABB Bomem, Quebec, Canada) utilized in this experiment was equipped with a tungsten-halogen source and an InGaAs diode array detector; in addition, a diffusive reflectance probe (FOCON FO; ABB Bomem) was connected to the spectrophotometer with a fiberoptic cable. NIR spectra of the reaction were continuously collected over a wave number range from 4,000 to 14,000 cm^{-1} at a resolution of 64 cm^{-1}. Each spectrum was recorded by averaging 16 scans, which took about 3 seconds. All NIR spectra were processed using the GRAMS/AI 7.00 software (Galactic Industries, Newark, NJ, USA), which was also used for data preprocessing, e.g., 2nd derivative calculations. Principal component analysis (PCA) was performed using the 'Unscrambler' software (CAMO Software AS, Oslo, Norway); a more detailed description of data analysis methods was previously published [23].

RESULTS AND DISCUSSION

1. Antisolvent Cocrystallization (30-Fold Scale-up)

As previously mentioned, the scaled-up process was optimized to manufacture highly pure cocrystal powder, which was accomplished using a fixed SAC/CBZ molar ratio of 1.6 [23]. Samples of the reaction mixture (volume=10 mL) were taken on a regular basis, beginning just after nucleation was observed and ending at 2 hours. Table 1 summarizes how the solid-mass balance changes over the course of this reaction. Specifically, the solid mass tends to increase as cocrystallization progresses; however, the solid content did not noticeably increase after 1 hour reaction time.

Although nucleation was observed after 3-8 minutes, samples of the solid mass taken from the sample after 5 minutes were too small to be weighed or measured via DSC or XRD. When the entire 4.5 L of reaction mixture was filtered and dried after 2 hours reaction time, a solid product weighing ≈3.5 g was measured, indicating an antisolvent cocrystallization yield of 73.4%. This value is comparable to our previous study accomplished at a much smaller scale [23].

Fig. 2 compares the change in XRD pattern of crystals produced under different water addition rates. Figs. 2(a) to 2(c) correspond to reactions occurring at 300, 900, and 100 mL/min water addition rates. Agitation was conducted at an intermediate mixing rate (300 rpm). As shown in Fig. 2(a), crystals sampled at 7 minutes are a mixture of three ingredients: CBZ hydrate and two CBZ-SAC cocrystal polymorphs (form-I and form-II). As the reaction pro-

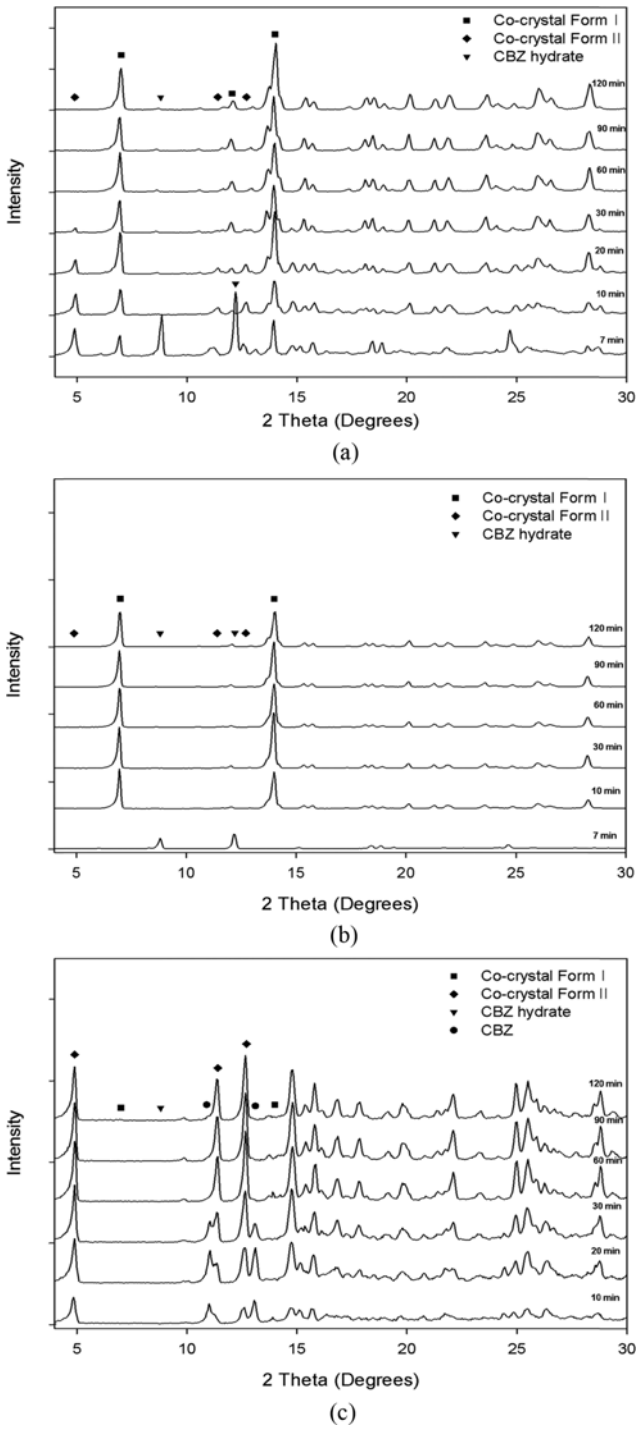

Fig. 2. XRD patterns for reactions using different water addition rates (all agitated at 300 rpm): (a) 300 mL/min, (b) 900 mL/min, and (c) 100 mL/min.

Table 1. Solid mass and yield for a process under intermediate kinematic conditions (@ 300 rpm and 300 mL/m)

Sample no.	1	2	3	4	5	6	7	Final product
Reaction time (m)	5	7	10	20	30	60	90	120
Solid mass (mg)	~0	22.2	28.2	29.4	33.7	33.5	33.8	3,461
Solid yield (%)								73.4

ceeded, the form-I peak increased, while the other peaks became lower. In particular, the CBZ hydrate peak disappeared within a few minutes. After 1 hour, only the form-I was present, as the form-II peak had disappeared completely.

When the water addition rate was increased threefold, we observed a significant change in the cocrystallization pathway compared to that in Fig. 2(a). As shown in Fig. 2(b), no CBZ-SAC cocrystal phases were observed within the initially formed CBZ hydrates. These transient CBZ hydrate particles were rapidly transformed to form-I cocrystals within 10 minutes.

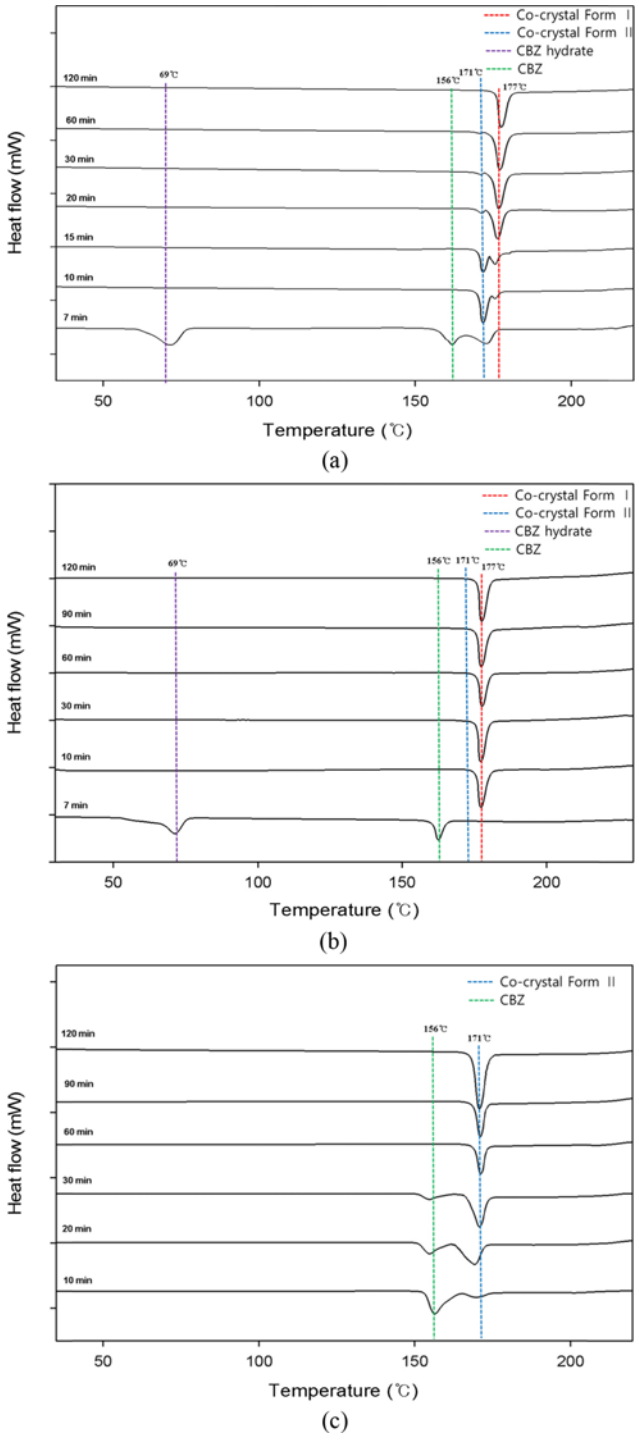

Fig. 3. DSC thermograms for reactions under different water addition rates (agitated at 300 rpm): (a) 300 mL/min, (b) 900 mL/min, and (c) 100 mL/min.

As shown in Fig. 2(c), when water was added slowly (at a rate of 100 mL/min), no peaks corresponding to either the cocrystal form-I or CBZ hydrates were observed; instead, CBZ and CBZ-SAC cocrystal form-II phases were detected. The crystalline phase noted in XRD patterns throughout the entire 2-hour reaction time corresponded to cocrystal form-II. As the reaction progressed, peak intensities also increased. Therefore, a slower addition of the antisolvent (water) to the methanol solution containing CBZ and SAC strongly modified the reaction pathway to favor the cocrystal form-II.

These same water addition rate effects were also noted by DSC, as summarized in Fig. 3. When the water addition rate was 300 mL/m (Fig. 3(a)), the first DSC thermogram taken at 7 minutes included three apparent peaks at around 69, 156, and 171 °C. The first two peaks were attributable to the presence of CBZ hydrates [27]; an endothermic peak would be associated with the cocrystal form-II. Contrary to results shown in Fig. 2(a), cocrystal form-I phases were not detected. After a few minutes, the DSC peaks at 69 and 156 °C disappeared, and a new peak at 177 °C was noted, which corresponded to the formation of cocrystal form-I. As cocrystallization proceeded, the peak at 171 °C decreased as the peak at 177 °C increased. At the end of cocrystallization, one prominent peak at 176 °C, corresponding to the cocrystal form-I, was left. This interpretation is nearly identical to the one presented in Fig. 2(a).

Under a faster water addition rate (900 mL/min), all the DSC thermograms indicated the existence of pure cocrystal form-I, except for the one taken at 7 minutes (Fig. 2(b)), which indicated that two endothermic peaks occurred at 69 and 156 °C, corresponding to the CBZ hydrate. Hence, crystallization can be presumed to be initiated by the formation of CBZ hydrate nucleates, followed by the transformation to cocrystal form-I with subsequent crystal growth. This is in a good agreement with experimental results shown in Fig. 2(b). Thus, the formation of cocrystal form-I is preferred to form-II when the water addition rate is 300 mL/min or greater.

Conversely, when water addition occurs at a rate less than 100 mL/min, a strong peak at 156 °C signals the initial crystallization process, which is associated with the formation of the CBZ phase. A weak peak at 171 °C was also detected, corresponding to the cocrystal form-II. Subsequent thermograms also showed two endothermic peaks until the 30-minute mark, which corresponded to the CBZ crystal and cocrystal form-II, respectively. After 30 minutes, only the form-II was present, and the CBZ peak was completely gone, which is consistent with the interpretation presented in Fig. 2(c).

Fig. 4 illustrates the characteristics of the final products prepared under two different conditions (Figs. 2, 3). Fig. 4(a) shows crystals formed under a faster water addition rate; these crystals are planar, matching the typical morphology of the CBZ-SAC cocrystal form-I, as reported in the literature [14]. In contrast, crystals formed under a slower water addition rate had a needlelike morphology, as shown in Fig. 4(b). This shape also matched previous observations for CBZ-SAC cocrystal form-II crystals [14]. Therefore, we were able to control for the formation of two cocrystal polymorphs

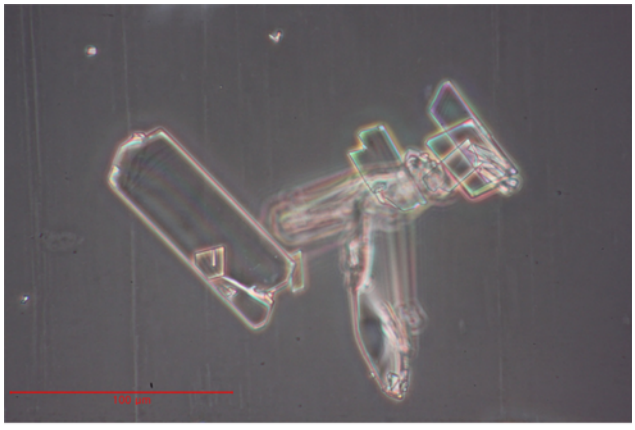

(a)

(b)

Fig. 4. Typical micrographics of CBZ-SAC cocrystal particles prepared under two contrasting conditions (agitated at 300 rpm): (a) water addition at 900 mL/min and (b) water addition at 100 mL/min.

by altering the antisolvent addition rate.

We also carried out similar experiments, except by changing the agitation speed. The results from the agitation speed were less pronounced than for the water addition rate; hence, these results were analyzed together. The variability in polymorphism, as dependent on water addition rate and agitation, is summarized in a simple three-dimensional (3-D) plot in Fig. 5. A slower water addition rate (100 mL/min) resulted in the presence of cocrystal form-II from nucleation to the end of the reaction. When the addition rate was increased to 300 mL/min, three phases (CBZ-hydrate, and cocrystal form-I and form-II) were initially formed. In this case, however, the hydrate and form-II disappeared when cocrystallization was dominated by form-I, resulting in pure form-I. When the addition was performed at a rate of 900 mL/min, the initial reaction was dominated by CBZ hydrates, and subsequently by form-I.

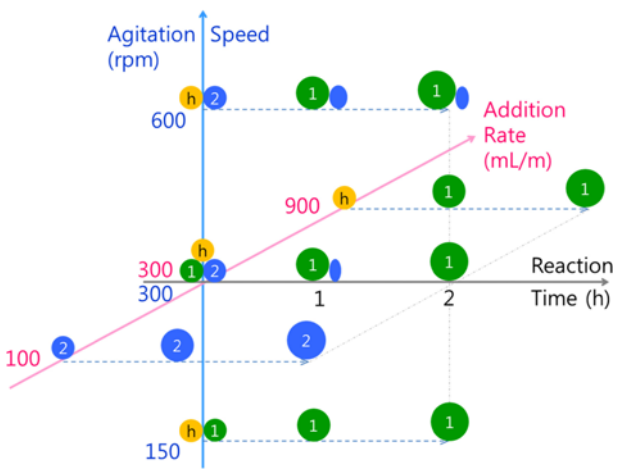

Fig. 5. A schematic 3-D plot showing the effects of kinetic parameters on cocrystallization.

When the rate of antisolvent addition is increased, one expects the local supersaturation to increase. Accordingly, initial nucleation is dominated by the CBZ hydrates, which are known to be favorable under highly hydrous conditions [23]. We anticipated that nucleation is dominated by the cocrystal form-I if water is added slowly, primarily because form-I is the stable polymorph over the meta-stable cocrystal form-II [14]. Notably, the initial solid sample observed contained CBZ and cocrystal form-II when performed at the slowest water addition rate. Moreover, we were unable to detect crystalline phases of form-I at any time during the 2-hour cocrystallization process.

The formation of form-II should be favored under low supersaturation conditions with respect to the initial reactants and cocrystal form-I, which can be explained because even though form-II is a less stable polymorph than form-I, their differences in water solubility are marginal (Table 2) [26]. Form-II, however, is much less soluble in methanol than form-I. Therefore, as water is slowly introduced into the methanol solution, nucleation of the cocrystal form-II is favored over form-I or CBZ hydrates. Based on this observation, further slowing the water addition rate would likely allow form-II to dominate the antisolvent cocrystallization reaction in a methanol-water system.

In regard to the effects of changing the agitation speed, the results on cocrystal and polymorph formation were less distinct. When the agitation was slower than 150 rpm, with a water addition rate fixed at 300 mL/min, the initial crystallization was dominated by CBZ hydrates and cocrystal form-I. As the agitation speed increased, the initial stage nucleation tended to move toward favoring form-I to form-II. The effect of agitating the solution faster should be equivalent to a slower antisolvent addition rate, which should result in a lower degree of local supersaturation. Nevertheless, the effect of the agitation rate on polymorphic selection was not strong. A system capable of agitating faster than the mechanical impeller may

Table 2. Solubility data for CBZ and its two co-crystal polymorphs [26]

Solvent	Solubility (mole/L)			
	CBZ	SAC	Form-I	Form-II
Water	0.0004	0.015	0.006	0.007
Methanol	0.264	0.389	0.895	0.373
Ethanol	0.080	0.268	0.454	0.202
DMSO	0.345	5.397	2.727	4.025

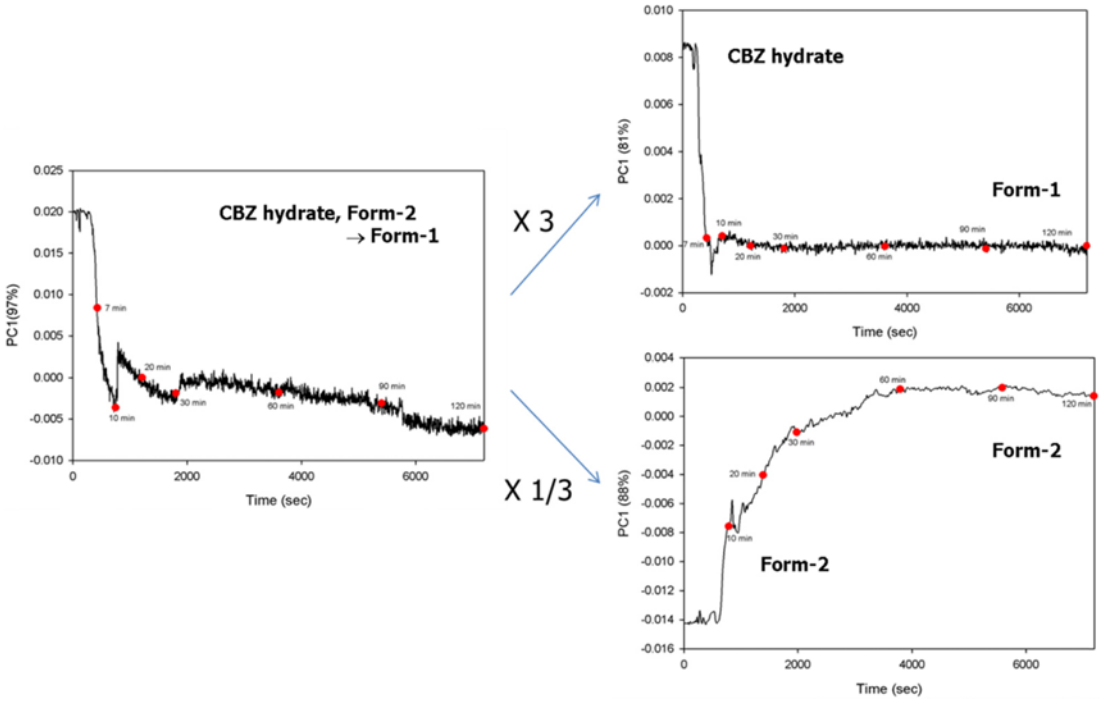

Fig. 6. The effect of water addition rate on the PC1 profile versus reaction time.

be necessary to more thoroughly examine this proposition.

Another factor that needs to be considered to further examine the potential for scaling up this reaction includes the direction of solvent addition, which has been shown to affect cocrystal formation, polymorphic selection, and transformation during antisolvent cocrystallization.

2. Analysis of In-line Monitoring Results Using Principal Components Analysis (PCA)

Fig. 6 summarizes the analysis of NIR-based in-line monitoring using PCA. Plots of PC1 scores versus reaction time at various water addition rates are shown. As the PC1 score encompassed the greatest degree (86-97%) of the total spectral variation for each of the cocrystallization experiments, we can presume that most of the variability in the cocrystallization process is explained by PC1 scores.

As the two extreme water addition rate conditions resulted in a rather simple and monotonous change in PC1 score, we first examined them. When water was added at 900 mL/min, the PC1 score dropped at ~3 minutes, followed by a small increase at ~8 minutes. As shown in Fig. 5 as well as XRD/DSC plots in Figs. 2 and 3, the fast initial drop in PC1 score was associated with the formation of CBZ hydrate particles. The subsequent small increase in PC1 score was caused by the swift transformation of CBZ hydrate nucleates to cocrystal form-I crystallites. Then, the PC1 score plateaued despite crystal growth. Therefore, the growth of CBZ–SAC form I cocrystals did not significantly affect the PC1 score at the end of cocrystallization.

When water was added slowly (100 mL/min), the PC1 score was uniformly low until 7 minutes, at which time it increased dramatically. The increase appears to match the formation of CBZ and CBZ-SAC cocrystal form-II nucleates. This profile plateaued after an hour, which indicated that nucleation was insignificant, with cocrystal growth dominating between 60 and 120 minutes reaction time.

When water was added at an intermediate rate of 300 mL/min (left plot in Fig. 6), the PC1 score remained at a maximal value, falling quickly at 5 minutes. The PC1 score then increased at 10 minutes, again falling after a minute; it then decreased gradually (with small variations) until the end of the crystallization process. If these trends are combined with the XRD patterns and DSC thermograms shown in Fig. 2 and Fig. 3, one can surmise that the first large drop in PC1 score can be attributed to the formation of CBZ-SAC form-II, as well as CBZ hydrate particles during nucleation.

3. Interpretation of Kinetic Parameters

Table 2 shows the solubility values of chemicals involved in the cocrystallization process, as reported in the literature [26]. The cocrystal form-I is less soluble than the form-II in water, but the reverse is true in methanol, the solvent used our antisolvent study. Therefore, solubility competition is dependent not only the ratio between water and methanol, but also conditions such as the rate of water addition.

Fig. 7 summarizes our cocrystallization study. Based on typical water addition rate values, conditions can be divided into three regimes: a low rate (e.g., 100 mL/min), an intermediate rate (e.g., 300 mL/min), and a fast rate (e.g., 900 mL/min). Under a fast addition rate, an extraordinarily high degree of supersaturation leads primarily to nucleation dominated by CBZ hydrate, over that of cocrystal form-I or form-II particles. As water is mixed uniformly with methanol, nucleates of CBZ hydrate transform to CBZ-SAC form-I particles by combining with dissolved SAC. Cocrystallization is completed by the subsequent growth of form-I crystals.

When water is added slowly, the local degree of CBZ and SAC supersaturation is relatively low. In this case, the form-II phase is preferred due to its lower solubility in a methanol solution com-

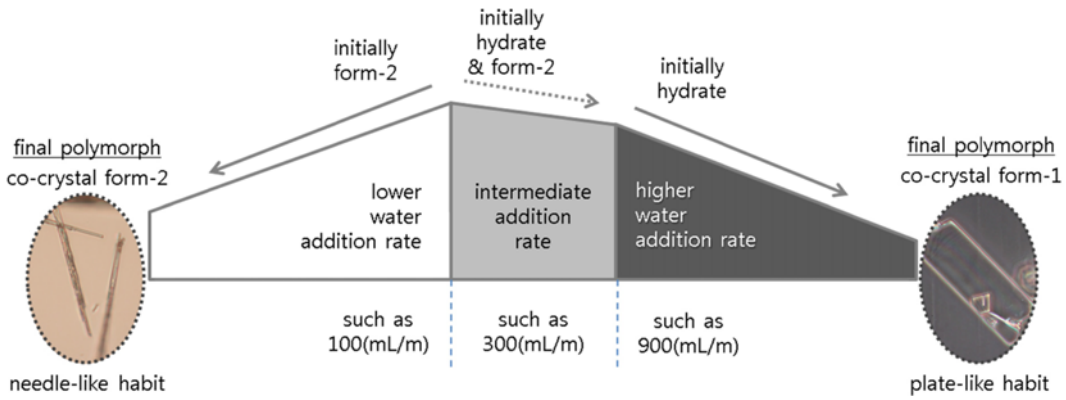

Fig. 7. A schematic showing the effects of changing water addition rates on the formation of CBZ-SAC cocrystals.

pared to form-I, as shown in Table 2. In this case, cocrystallization is controlled and terminated completely as form-II.

If this process is performed under an intermediate water addition rate (e.g., 300 mL/min), nucleation involves the formation of CBZ hydrate and cocrystal form-II particles together. In this case, CBZ hydrate particles quickly covert to form-I, leading to subsequent crystal growth. Additionally, form-II nucleates transform gradually to form-I, presumably via SMPT. After ~40 minutes, the slurry solution included only form-I particles.

A series of studies for the mechanism of CBZ-SAC cocrystal polymorph selection is under way. In this study, the relationship between the solvent-water composition and the solubility values of two cocrystal polymorphs is taken into account. For more comprehensive understanding, methanol and ethanol are being studied at various ratios in solvent/water mixtures.

CONCLUSIONS

We have presented a study on variables affecting the large-scale antisolvent manufacture of carbamazepine-saccharin (CBZ-SAC) cocrystals. Although two polymorphs have been known to form during the stable phase of crystallization, adjusting the SAC/CBZ ratio or water/methanol ratio was previously reported to selectively produce the polymorph form-I or form-II [26]. In addition to these chemical composition conditions, we found that conditions such as the addition rate of an antisolvent and agitation speed can play a major role in determining which CBZ-SAC cocrystal forms, especially during a large-scale reaction.

According to sampling during the cocrystallization reaction, form-I was preferably formed as the addition rate or agitation speed increased. Under the opposite conditions, nucleation and crystal growth was instead dominated by form-II, which was also valid for chemical conditions that were recently reported to produce pure cocrystal form-I. From a stability test (accomplished by heating the form-I and form-II cocrystal powders at 70 °C for 4 weeks), both polymorphs were very stable with no noticeable polymorphic transformation or degradation. Consequently, kinetic process parameters should be considered as a potential means of tuning reactivity when a specific cocrystal polymorph is desired via antisolvent methods. Also, we demonstrate here that in-line NIR measurements can be useful toward monitoring the reaction pathways of solution-based cocrystallization processes.

ACKNOWLEDGEMENTS

This work was supported by the Soon Chun Hyang University Research Fund (No. 20130607).

REFERENCES

1. FDA, Guidance for industry; Regulatory classification of pharmaceutical co-crystals, http://www.fda.gov/Drugs/GuidanceComplianceRegulatoryInformation/Guidances/default.htm (2013).
2. N. J. Babu and A. Nanjia, *Cryst. Growth Des.*, **11**, 2662 (2011).
3. N. Qiao, M. Li, W. Schlindwein, N. Malek, A. Davies and G. Trappitt, *Int. J. Pharm.*, **419**, 1 (2011).
4. H. G. Brittain, *J. Pharm. Sci.*, **102**, 311 (2013).
5. J. W. Steed, *Trend Pharmacol. Sci.*, **34**, 185 (2013).
6. R. Thakuria, A. Delori, W. Jones, M. P. Lipert, L. Roy and N. Rodríguez-Hornedo, *Int. J. Pharm.*, **453**, 101 (2013).
7. L. Padrela, M. A. Rodrigues, S. P. Velaga, H. A. Matos and E. G. deAzevedo, *Eur. J. Pharm. Sci.*, **38**, 9 (2009).
8. J. H. ter Horst and P. W. Cains, *Cryst. Growth Des.*, **8**, 2537 (2008).
9. R. S. Dhumal, S. V. Biradar, A. R. Paradkar and P. York, *Int. J. Pharm.*, **368**, 129 (2009).
10. A. Alhalaweh and S. P. Velaga, *Cryst. Growth Des.*, **10**, 3302 (2010).
11. J. H. ter Horst, M. A. Deij and P. W. Cains, *Cryst. Growth Des.*, **9**, 1531 (2009).
12. K. Yamamoto, S. Tsutsumi and Y. Ikeda, *Int. J. Pharm.*, **437**, 162 (2012).
13. P. P. Bag, M. Patni and C. M. Reddy, *CrystEngComm*, **13**, 5650 (2011).
14. W. W. Porter III, S. C. Elie and A. J. Matzger, *Cryst. Growth Des.*, **8**, 14 (2008).
15. T. K. Wu, S. Y. Lin, H. L. Lin and Y. T. Huang, *Bioorg. Med. Chem. Lett.*, **21**, 3148 (2011).
16. D. J. Good and N. Rodriguez-Hornedo, *Cryst. Growth Des.*, **9**, 2252 (2009).
17. A. B. M. Buanz, G. N. Parkinson and S. Gaisford, *Cryst. Growth Des.*, **11**, 1177 (2011).
18. W. Limwikrant A. Nagai, Y. Hagiwara, K. Higashi, K. Yamamoto and K. Moribe, *Int. J. Pharm.*, **431**, 237 (2012).

19. T. Rager and R. Hilfiker, *Cryst. Growth Des*., **10**, 3237 (2010).
20. G. D. Profio, V. Grosso, A. Caridi, R. Caliandro, A. Guagliardi, G. Chita, E. Curcio and E. Drioli, *CrystEngComm*, **13**, 5670 (2011).
21. A. Caridi, G. Di Profio, R. Caliandro, A. Guagliardi, E. Curcio and E. Drioli, *Cryst. Growth Des*., **12**, 4349 (2012).
22. A. Y. Sheikh, S. A. Rahim, R. B. Hammond and K. J. Roberts, *CrystEngComm*, **11**, 501 (2009).
23. I.-C. Wang, M.-J. Lee, S.-J. Sim, W.-S. Kim, N.-H. Chun and G. J. Choi, *Int. J. Pharm*., **450**, 311 (2013).
24. M.-J. Lee, N.-H. Chun, I.-C. Wang, J. J. Liu, M.-Y. Jeong and G. J. Choi, *Cryst. Growth Des*., **13**, 2067 (2013).
25. N.-H. Chun, I.-C. Wang, M.-J. Lee, Y.-T. Jung, S.-k. Lee, W.-S. Kim and G. J. Choi, *Eur. J. Pharm. Biopharm*., **85**, 854 (2013).
26. S. K. Pagire, S. A. Korde, B. R. Whiteside, J. Kendrick and A. Paradkar, *Cryst. Growth Des*., **13**, 4162 (2013).
27. E. Lu, N. Rodríguez-Hornedo and R. Suryanarayanan, *CrystEngComm*, **10**, 665 (2008).